GEOMETRY INFLUENCE OF THE MICRO ALKALI VAPOR CELL ON THE SENSITIVITY OF THE CHIP-SCALE ATOMIC MAGNETOMETERS

Yu Ji, Qi Gan, Lei Wu and Jintang Shang
Key Laboratory of MEMS of Ministry of Education, Southeast University, Nanjing, China

ABSTRACT

This paper focuses on geometry influence of the micro alkali vapor cell on the sensitivity of the chip-scale atomic magnetometers. For the first time, by using micro spherical alkali vapor cells instead of traditional micro planar alkali vapor cells, we demonstrate a chip-scale atomic magnetometer with a ten-fold improvement in sensitivity experimentally. Besides, results also show that the micro spherical cell has improved anti-relaxation properties, especially at low buffer gas pressure. The geometry of the micro vapor cell might also be important for the performance of other chip-scale atomic devices including chip-scale atomic clocks, vector atomic microwave electrometers and atomic gyroscopes.

INTRODUCTION

Benefiting from techniques of Micro-Electro-Mechanical-Systems (MEMS), chip-scale atomic magnetometers characterized by small size, low power consumption and low fabrication cost have a greatly broadened applications. For instance, compared with conventional superconducting quantum interference devices (SQUIDS) and large scale atomic magnetometers, chip-scale atomic magnetometers can be used more conveniently in space exploration[1-2], geomagnetic mapping[3], perimeter and remote sensing[4], bio-magnetic applications[5] and some applications of the internet of things[6].

Compared with large-scale atomic magnetometer using macro (about few cm) alkali vapor cells, chip-scale atomic magnetometers have much lower sensitivity[4]. For chip-scale atomic magnetometers, the most radical solution for improving performance is to reduce relaxation rates of the atomic ground-state polarization. Collisions of the alkali atoms against the cell walls become much more rigorous with the decrease of the alkali vapor cell sizes, which destroy the atomic ground-state polarization. Buffer gases and anti-relaxation wall coatings has been taken to improve the performance of chip scale atomic magnetometers. Alkali vapor cell geometry also plays an important role of chip-scale atomic magnetometers [7]. In the micro scale, how the geometry of the alkali vapor cell affects the performance of the chip scale magnetometers has not been disclosed.

The conventional micro alkali vapor cells[8-9] for chip-scale atomic magnetometers are usually fabricated with a glass-silicon-glass sandwich structure based on techniques of micro-electro-mechanical systems (MEMS). However, as shown Fig.1, due to the small thickness of the double polished silicon wafer ranged from 300um to 1mm[8-9], alkali atoms in the conventional micro planar alkali vapor cell suffer from frequent wall collisions, especially in the low buffer gas pressure. Besides, optical path length of the conventional micro planar alkali vapor cell is relatively low. Based on the previous research of the corresponding author's group[11-12], this paper focuses on the geometry influence of the vapor cells on the performance of the chip-scale atomic magnetometer experimentally. In order to overcome the shortcomings of the conventional micro alkali vapor cells and improve the sensitivity of chip-scale atomic magnetometers, we designed and fabricated wafer-level micro spherical rubidium vapor cells for chip-scale atomic devices. In the following parts, we will firstly design and fabricate micro vapor cells of planar and spherical shapes. Then characterization and comparison of the two types of vapor cells will be performed in chip-scale atomic magnetometers using Mz techniques[3].

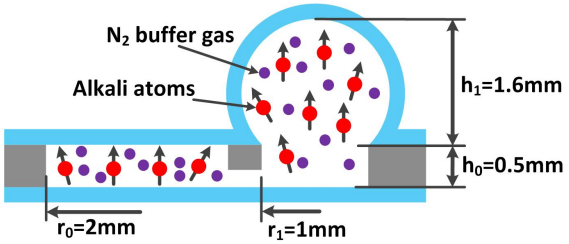

Figure 1: A schematic cross-sectional view of the micro cells equipped with one spherical chamber and one planar chamber. The two cells are designed with the same volume of about 6mm^3.

CELL DESIGN AND FABRICATION

For comparison and characterization, we designed interconnected planar and spherical vapor cells of the same volume to get equal inner gas pressure (Fig.1). As shown in Fig.1, according to the equation of the micro spherical cell[11]:

$$V_1 = \pi r_1^2 h_0 + \frac{\pi h_1 (3r_1^2 + h_1^2)}{6}, \qquad (1)$$

it can be easily calculated that the volume of the micro spherical cell equals to 6.22mm^3. The volume of the micro planar cell equals to $\pi r_0^2 h_0$, which is approximately 6.28mm^3, In the vapor cells, nitrogen was used as the buffer gas to reduce the wall collisions.

Fabrication of the micro vapor cells was conducted on wafer-level, which is depicted as follows (Fig.2). Firstly, based on the previous research[11-12], wafer-level micro glass bubbles were prepared by a chemical foaming process (CFP) and a hot forming process (HFP). The volume of the micro glass bubbles was controlled accurately, as shown in Fig.2.(a). Secondly, micro spherical cells interconnected with micro planar chamber by micro channels were formed on the back side of the bonded wafers by dry etching with SF_6 and O_2 (Fig.2.(b)). Then, a glass wafer was bonded to seal the wafer-level

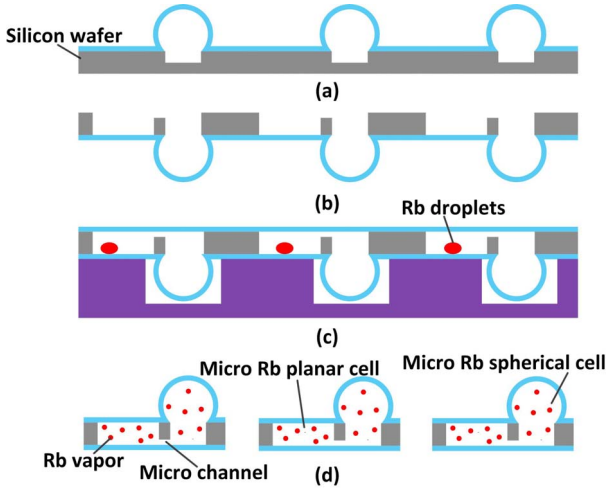

Figure 2: Fabrication process of the wafer-level micro cells equipped with one spherical chamber and one planar chamber. (a) Preparing glass bubbles combing chemical foaming process(CFP) and hot forming process(HFP); (b) Dry etching to form the micro spherical chamber, micro planar chamber and micro channel; (c) Anodic bonding to seal the wafer and introducing rubidium droplets and nitrogen buffer gas; (d) Dicing the wafer into individual one.

micro cells (Fig.2.(c)). Before the sealing, rubidium and buffer gas were filled in the vapor cells. At last, the bonded wafers were divided into individual ones (Fig.2(d)). From the photograph of the individual micro alkali vapor cell, it is shown that there are rubidium droplets visible in the enlarged photograph below (Fig.3). Besides, cells of three different nitrogen buffer gas pressure were fabricated. The optical absorption lines was broadened to 3.6GHz, 16GHz and 42GHz full-width at half-maximum corresponding to 0.2amg, 0.88amg and 2.35amg nitrogen gas pressure respectively, calculated by rubidium data from M. V. Romalis *et al*[13].

CHARACTERIZATION OF SIGNAL STEEPNESS AND SENSITIVITY

In this paper, chip-scale atomic magnetometer by using techniques of Mz was used for the characterization of the micro cells[3]. As shown in Fig.4, the Mz magnetometer had several components: a vertical cavity surface emitting Laser(VCSEL), a lens, a quarter-wave plate, a micro vapor cell integrated with heater, helmholtz coils and photo-detector. Pumping and probing laser was generated by the VCSEL with a typical linewidth below 100MHz. After the light emitting from the VCSEL had passed through the quarter-wave plate, the circularly polarized laser beam went into the micro rubidium vapor cell. The first helmholtz coils placed in the horizontal direction are used to generate a homogeneous static magnetic field in the direction of optical beam propagation as a standard magnetic field for testing. The second helmholtz coils placed in the vertical direction were used to generate a RF magnetic field to induce resonant coherent precession of the polarized atomic spins. Meanwhile by using the second Helmholtz coils, modulation of the oscillation frequency ω at low frequency Ω_m, accompanied with the synchronous detection of the signal at the same

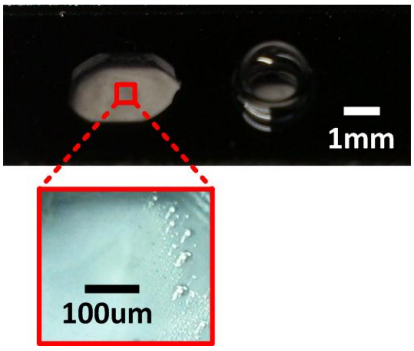

Figure 3: Photograph of the micro cell equipped with one planar chamber and one spherical chamber, rubidium droplets are visible in the zoom-out photograph below.

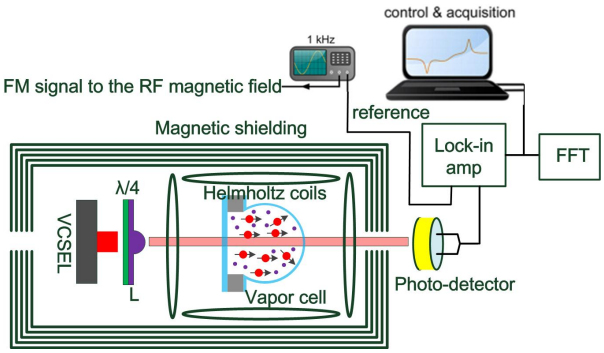

Figure 4: Experimental setup of atomic magnetometer using Mz techniques.

frequency Ω_m, was used for lock-in detection of the opticalpolarization signal. The vapor cell integrated with micro heater was heated by 100KHz AC electronic current in order to avoid external magnetic noise. After the light penetrated the micro vapor cell, the optical polarization signal is detected via a photo-detector. The amplified photo-current signal is then mixed with the modulator reference Ω_m in a one-channel lock-in-amplifier and recorded with a computer based high resolution data acquisition system to get the dispersive signal.

The magnetometer is housed inside a five layer cylindrical magnetic shield and the magnetic filed is extracted by measuring Larmor frequency. The use of radio-frequency excitation to measure Larmor frequency was first proposed by Dehmelt[14]. In this paper, the RF field with amplitude of 160nT was used, and the low modulation frequency was 80Hz. By adjusting the oscillation frequency of the RF magnetic field from 12KHz to 36KHz, dispersive signal obtained from the micro rubidium vapor cells was observed. The magnetometer frequency response curves as shown in Fig.4 have two resonance spots because rubidium used in the vapor cells has two isotopes (for ^{85}Rb I=5/2 and for ^{87}Rb I=3/2). For rubidium atoms, the electron and nuclear spins of the atom act as coupled oscillators resulting in slower precession than a brae electron, and the gyromagnetic ratio of the atom is given by:

$$\gamma = \frac{\gamma^e}{2I+1} \tag{2}$$

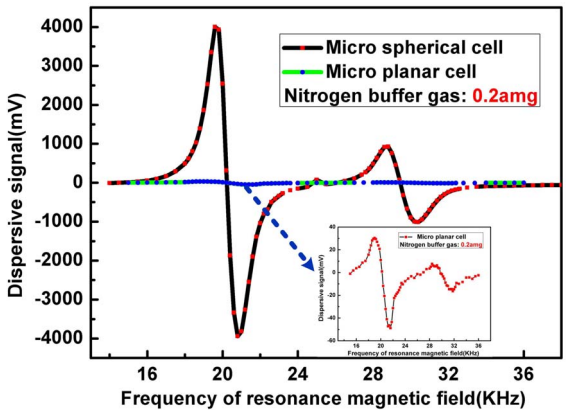

(a)

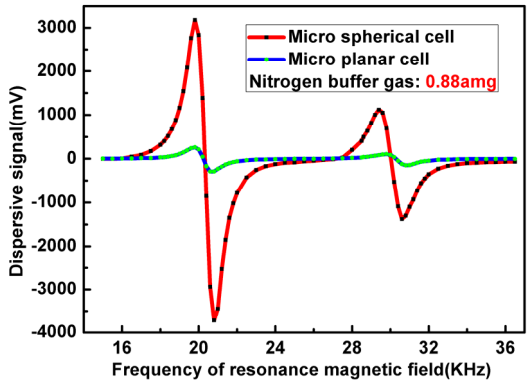

(b)

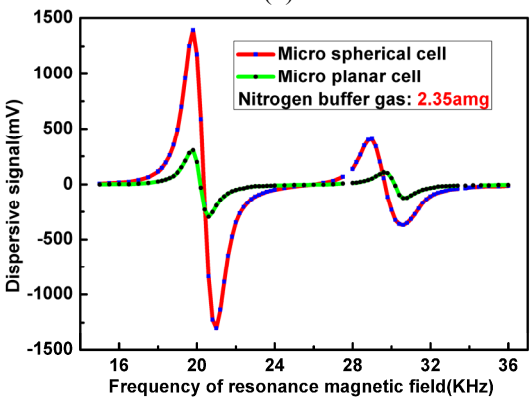

(c)

Figure 5: Dispersive signal of the three cells, test temperature is 80 degree centigrade. (a) Dispersive signal of the spherical and planar cell with 0.2amg buffer gas; (b) Dispersive signal of the spherical and planar cell with 0.88amg buffer gas;(c) Dispersive signal of the spherical and planar cell with 2.35amg buffer gas.

where the gyromagnetic ration of the bare electron equals to 28Hz/nT, therefore the gyromagnetic ratio of ^{85}Rb and ^{87}Rb is 4.67Hz/nT and 7Hz/nT respectively. As a result, ^{85}Rb and ^{87}Rb atoms have their own Larmor frequencies corresponding to about 20kHz and 30kHz. What's more, because ^{85}Rb accounts for 72.15% in natural rubidium and ^{87}Rb for 27.85%, the ^{85}Rb vapor density is approximately 2.6 times larger than the ^{87}Rb vapor density in the cells, therefore from the Fig.5, we could find that ^{85}Rb corresponding to 20kHz induces a stronger dispersive signal.

In this paper, three cells with different N_2 buffer gas pressure of 0.2amg, 0.88amg and 2.35amg were characterized. For the vapor cell having 0.2amg N_2 buffer gas, as shown in Table.1, atomic magnetometer using the micro spherical cell has a strong resonance signal and the signal steepness dS(w)/dw at the center of the resonance is 11.025V/KHz（as shown in Fig.5(a). Besides, the magnetic linewidth of ^{85}Rb resonance for the micro spherical cell is 1KHz. However, signal of the magnetometer using the micro planar cell is much lower. The inset figure in Fig.5.(a) is the rescaled resonance signal of the micro planar cell. The signal steepness *dS(w)/dw* at the center of the resonance is only 0.057V/KHz and the magnetic linewidth of ^{85}Rb resonance is 2.2KHz . The signal steepness *dS(w)/dw* for the micro spherical cell is approximately 193 times larger than the micro planar cell. At a buffer gas pressure of 0.88amg, as shown in Fig.5(b), the signal steepness *dS(w)/dw* at the center of the resonance for the micro spherical and planar cell is 10.812V/KHz and 0.962V/KHz. The signal steepness *dS(w)/dw* for the micro spherical cell is about 11.2 times larger than the micro planar cell. Similarly, for the cell with 2.35amg N_2 buffer gas, as shown in Fig.4(c), the signal steepness dS(w)/dw for the micro spherical cell is only 3.3 times larger than the micro planar cell.

Table 1: Comparison of the signal steepness dS(w)/dw at the center of the resonance

Buffer gas pressure	**The signal steepness *dS(w)/dw***		
	The spherical cell	**The planar cell**	**Ratio**
0.2amg	11.025V/KHz	0.057V/KHz	193
0.88amg	10.812V/KHz	0.962V/KHz	11.24
2.35amg	3.561V/KHz	1.071V/KHz	3.32

At low buffer gas pressure, since alkali atoms in the micro planar cell have much frequent wall collisions in the low buffer gas pressure, the signal steepness dS(w)/dw for the micro planar cell is weak and the magnetic linewidth is broad. With the increase of N_2 buffer gas pressure, the signal steepness *dS(w)/dw* of the micro spherical cell decreases because the absorption cross section is inversely proportional to the buffer gas pressure[15], while the signal steepness *dS(w)/dw* of the micro planar cell increases due to the decreased wall collisions. At high buffer gas pressure, wall collisions are much suppressed by the buffer gas and the micro spherical cell has much stronger resonance signal on account of increased optical path length. By comparison and analysis, it can be drawn that the micro spherical cell has improved signal steepness and anti-relaxation properties, especially at low buffer gas pressure.

At last, the sensitivity of the chip-scale atomic magnetometer was characterized and the cell with 0.88amg buffer gas was selected for comparison. As shown in Fig.6, magnetic field noise[16] at different temperatures ranging from 50 ℃ to 110 ℃ was characterized. At low temperatures, magnetometer has lower sensitivity due to the weak signal caused by low rubidium vapor density. With temperature increases, the sensitivity of magnetometer increases because of improved signal strength. However, at high temperatures, the sensitivity of

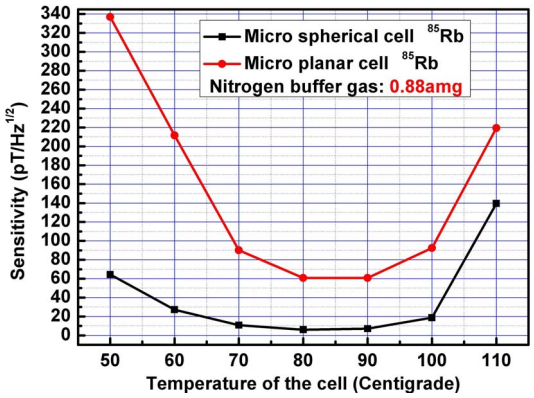

Figure 6: Comparison of the sensitivity of the micro spherical and planar cells for atomic magnetometers at different temperatures. The N_2 buffer gas pressure of the micro cell is 0.8amg.

magnetometer decreases rapidly because of the drastic spin exchange relaxations. For the cell with 0.88amg buffer gas, the optimal operation temperature is approximately 80℃. For ^{85}Rb resonance, under optimal conditions, chip-scale atomic magnetometer using the spherical cell has the sensitivity of 6pT/Hz$^{1/2}$ at 1Hz, while the device based on the planar cell is demonstrated with the sensitivity of 60pT/Hz$^{1/2}$ at 1Hz (Fig.6). The results demonstrate that chip-scale atomic magnetometers based on the micro spherical cell has a significantly improved sensitivity for chip-scale atomic magnetometers. We believe in the future, by using pure rubidium isotopes and decreasing measurement noise caused by electronic heating, the sensitivity of the chip-scale atomic magnetometer using micro spherical cell would be furtherly improved.

CONCLUSIONS

We focus on the geometry influence on the sensitivity of chip-scale atomic magnetometer and present wafer-level micro spherical rubidium vapor cells with signal steepness and sensitivity for chip-scale atomic magnetometer. For comparison and characterization, we designed a micro rubidium vapor cell interconnected with one spherical chamber and one planar chamber by a micro channel to acquire equal inner pressure. The two vapor cells are designed with the same volume of about 6mm^3. Chip-scale atomic magnetometers using the two vapor cells are used to evaluate the cell's performance. Three cells with different N_2 buffer gas pressure of 0.2amg, 0.8amg and 2.35amg are characterized. The dispersive signals obtained from the three different cells show that compared to the micro planar cells, the micro spherical cells have a greatly improved signal steepness *dS(w)/dw* at the center of the resonance, especially at low buffer gas pressure. With 0.88amg buffer gas at optimal conditions, chip-scale atomic magnetometer using the spherical cell has the sensitivity of 6pT/Hz$^{1/2}$ at 1Hz, while the device based on the planar cell is demonstrated with the sensitivity of 60pT/Hz$^{1/2}$ at 1Hz.

ACKNOWLEDGEMENTS

This work is supported by National Science Foundation of China (No. 51275091,No. 51675102). The funding for Specially-Appointed Professors by Universities in Jiangsu Province and "333 Projects" of Jiangsu Province are also acknowledged.

REFERENCES

[1] R. Mhaskar, S. Knappe, and J. Kitching, "A low power, high-sensitivity micromachined optical magnetometer", *Appl. Phys. Lett*., vol. 101, pp. 241105-1–241105-4, 2012.
[2] D. Sheng, S. Li, N. Dural and M. V. Romalis, "Subfemtotesla scalar atomic magnetometry using multipass cells", Phys. Rev. Lett., vol. 110, pp. 160802-1–160802-5, 2013.
[3] J. Kitching, S. Knappe, and E. A. Donley, "Atomic sensors–a review", *IEEE J. Sens*., vol. 11, pp. 1749-1758, 2011.
[4] D. Budker and M. Romalis, "Optical magnetometry", *Nat. Phys*., vol. 3, pp. 227-234, 2007.
[5] Jiménez-Martínez, Ricardo, et al, *Instrumentation and Measurement, IEEE Transactions on*, vol. 59, pp.372-378, 2010.
[6] S. Knappe, "MEMS atomic clock", *Compr.Microsyst.*, vol. 3 , pp. 571-612, 2008.
[7] D. Budker and D. F. J.Kimball, *Optical Magnetometry.* Cambridge University Press(2013), pp.127-129.
[8] L. A. Liew, S. Knappe, J. Moreland, H. Robinson, L. Hollberg and J. Kitching, "Microfabricated alkali atom vapor cells", *Appl. Phys. Lett*., vol. 84, pp. 2694-2696, 2004.
[9] L. A. Liew, J. Moreland and V. Gerginov,"Wafer-level filling of microfabricated atomic vapor cells based on thin-film deposition and photolysis of cesium azide", *Appl. Phys. Lett*., vol. 90, pp. 114106-1–114106-3, 2007.
[10] E. J. Eklund, A. M. Shkel, S. Knappe, E. Donley and J.Kitching, "Glass-blown spherical microcells for chip-scale atomic devices", *Sens. Actuators A, Phys*., vol. 143, pp. 175-180, 2008.
[11] J. Shang et al., "Preparation of wafer-level glass cavities by a low-cost chemical foaming process," *Lab Chip.*, vol. 11, no. 8, pp. 1532-1540, Mar. 2011.
[12] Y. Ji, Q. Gan, L. Wu, J. Shang, and C. P. Wong, "Wafer-Level Hermetic All-Glass Packaging for Microalkali Vapor Cells of Chip-Scale Atomic Devices", *IEEE Trans. Compon., Packag., Manuf. Technol*., vol. 5, no. 11, pp. 1551-1558, 2015.
[13] M. V. Romalis, E. Miron and G. D. Cates, "Pressure broadening of Rb D 1 and D 2 lines by ^{3}He, ^{4}He, N_2, and Xe: Line cores and near wings", *Phys. Rev. A*., vol. 56, pp. 4569-4578, 1997.
[14] Dehmelt, H. G. "Modulation of a light beam by precessing absorbing atoms." *Phys. Rev.*, vol.105, pp. 1924-1925, 1924.
[15] J. Vanier and C. Audoin, *The Quantum Physics of Atomic Frequency Standards,* Hilger, London, 1989.
[16] Kominis, I. K., Kornack, T. W., Allred, J. C., & Romalis, M. V. "A subfemtotesla multichannel atomic magnetometer." *Nature,* vol. 422, pp. 596-599, 2003.

CONTACT

*Jintang Shang, tel: +86 13913869603, Email: jshang@seu.edu.cn